

Letter to the Editor

Structural analysis of two novel mutations in *MCFD2* gene causing combined coagulation factors V and VIII deficiency

To the editor:

Combined factor V and factor VIII deficiency (F5F8D) is a rare autosomal recessive bleeding disorder reported usually in the context of consanguinous marriage. F5F8D is characterized by mild-to-moderate bleeding and coordinate reduction in plasma FV and FVIII levels, as well as platelet FV level (OMIM 227300) [1].

The disease is caused by mutations in genes encoding lectin mannose binding protein (LMAN1) and multiple coagulation factor deficiency 2 (MCFD2), which are the components of the endoplasmic reticulum (ER)-Golgi intermediate compartment (ERGIC-53) involved in the FV and FVIII intracellular transport [1, 2]. LMAN1 is a type-I integral membrane protein that was first described as a 53-kDa marker of the ERGIC [3], whereas MCFD2 is a soluble luminal protein

with 2-calmodulin-like EF-hand motifs. MCFD2 interacts with ERGIC-53 in a calcium-dependent manner, and the complex recycles between the ER and the ERGIC. The ERGIC-53/MCFD2 complex is believed to capture FV and FVIII in the ER and to package the two coagulation factors into transport vesicles that mediate transport to the ERGIC. Five of the previously reported MCFD2 missense mutations (D81Y, D89A, D122V, D129E and I136T) change the highly conserved amino acid residues of the first EF-hand domain and two mutations (D129E and I136T) have been shown to abolish LMAN1 binding, indicating that LMAN1 and MCFD2 must function as a unit to transport FV and FVIII [4].

Here we report for the first time a case of F5F8D disorder in a Tunisian family, resulting from two novel mutations in exon 3 of the *MCFD2* gene. The structural consequences of the novel mutations (V100D and D81H) in MCFD2 protein were evaluated by extensive molecular dynamics simulations using GROMACS 3.0 software [5], similar to our previous study of other protein–ligand systems [6].

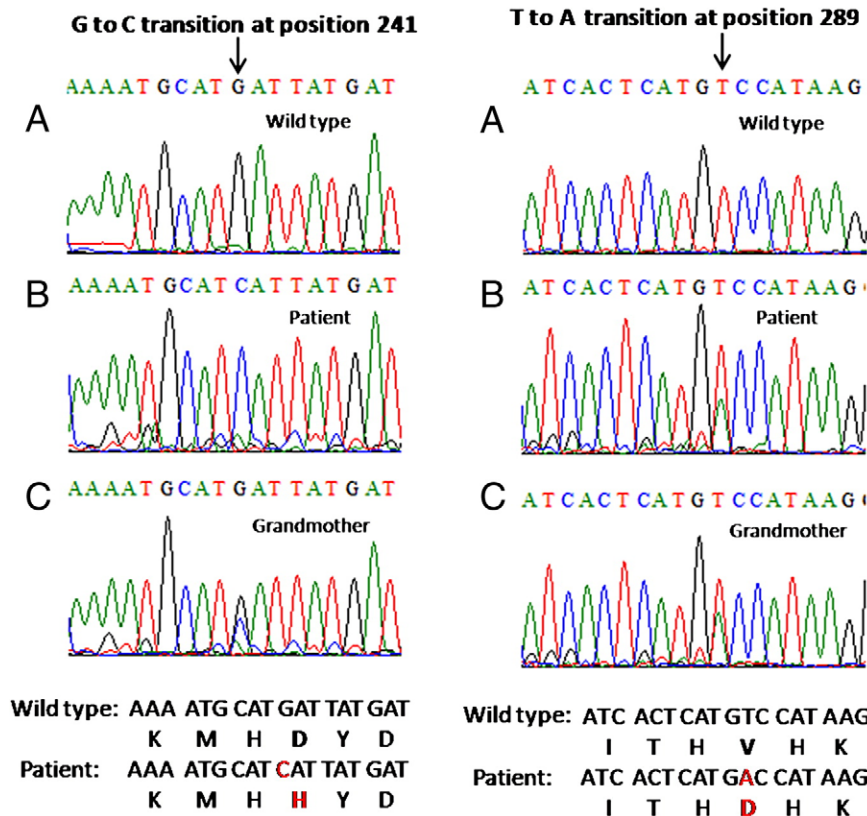


Fig. 1. DNA sequence surrounding nucleotides 241 and 289 of *MCFD2* exon 3. (A) DNA sequence of the normal control. The normal nucleotides (G and T) are indicated by an arrow. (B) DNA sequence of the patient, a homozygous mutation G to C transition at nucleotide 241, which causes Asp81His mutation, and a heterozygous mutation T to A transition at nucleotide 289, which causes Val100Asp mutation, are present. (C) DNA sequence of the patient's paternal grandmother, G to C and T to A transitions are present in the heterozygous state.

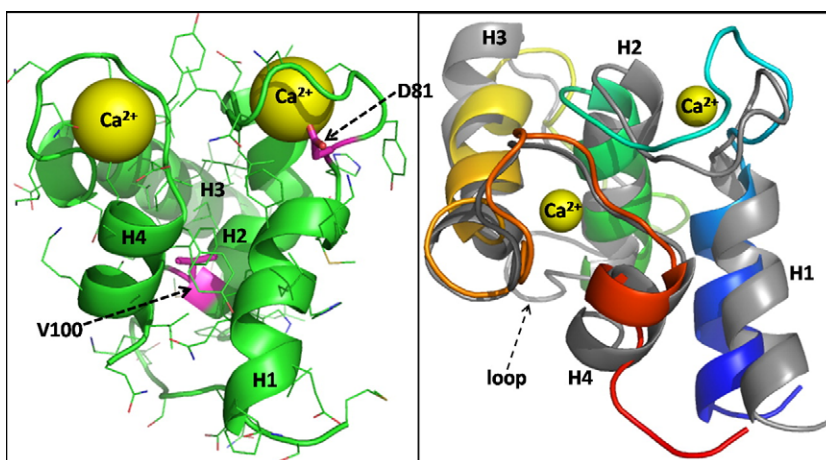


Fig. 2. (Left) Ribbon view of the human MCFD2 NMR structure with the positions of the mutant residues (D81 and V100). (Right) Superposition of the averaged MCFD2^{D81H-V100D} structure with the wild-type MCFD2^{wt} (gray color) obtained from the MD simulation. The Ca²⁺ of both EF-hand domains is shown in yellow balls.

A three-year-old boy, born of consanguineous marriage, was presented to the hematology service at the Aziza Othmana Hospital, Tunisia. A hemostatic test that was conducted as an assessment before repairing a right inguinal hernia and performing a circumcision revealed a prolonged PTT and PT as a result of decreased FV (14%) and FVIII (5%). The patient was operated under substitutive treatment (FFP) and factor FVIII concentrate, and a hemorrhagic syndrome post-circumcision was observed 1 week post-operative. Blood samples were obtained from the affected patient and his grandmother. Genomic DNA was prepared from whole blood using a commercial DNA extraction kit (QiaAmp, Qiagen, Crawley, UK). The LMAN1 and MCFD2 coding regions, including intron-exon boundaries, were amplified by polymerase chain reaction (PCR).

Results: Direct DNA sequencing of all amplified fragments detected no mutations in patient's LMAN1 gene, whereas sequence analysis of the *MCFD2* gene revealed the presence of a double mutation. Patient was homozygous for the first mutation localized in exon 3, which corresponded to the transition G→C at nucleotide 241. The transition caused the substitution Asp81→His of MCFD2 protein. Furthermore, the patient was heterozygous for the second mutation, localized in exon 3 of the same gene, which corresponded to the transition T→A at nucleotide 289. The transition subsequently mutated the Val100→Asp residue of the MCFD2 protein (Fig. 1). The paternal grandmother of the patient was heterozygous for these two mutations. Since the grandmother is healthy, it appears that both mutations belong to the same allele of the *MCFD2* gene (genotype: double heterozygous +/241_289). Patient inherited the double-mutated alleles at positions 241–289 from his paternal grandmother and a single mutated allele at position 241 from his mother. Therefore, the patient's genotype is 241_+/241_289.

The solution structure of human wild-type MCFD2^{wt} protein has already been determined by NMR spectroscopy [7] and was used to build the MCFD2^{D81H-V100D} mutant. The overall structure of MCFD2^{wt} is composed of four α -helices and two short β -sheets. As predicted from sequence homology, these secondary structure elements form two EF-hand domains, which interact with each other to give an overall fold similar to the C-terminal domain of human calmodulin (Fig. 2) [8].

To examine the effect of the mutations on the global structure, we calculated the root mean square deviation (C α -RMSD) and time evolution of the secondary structure of both MCFD2^{wt} and MCFD2^{D81H-V100D} proteins through the MD simulations. The MD trajectory confirmed that the MCFD2^{wt} structure was very stable (Fig. 3), with a C α -RMSD that remained almost intact during ~20 ns of MD simulation. As expected, the full-length MCFD2^{wt} displayed a

quite high RMSD fluctuation of ~2.5 Å during the simulation, reflecting the general conformational flexibility of the unstructured region (residues 102–113) of the protein. Interestingly, the C α -RMSD of the residues involved in secondary structure and both EF-hand domains converged to ~1.5 Å, indicating that the hydrophobic core of MCFD2^{wt} structure was stable and compact during the simulation. Furthermore, the MCFD2^{wt} secondary structure elements were well preserved and fairly stable for the period of simulation (Fig. 4). Thus, the conformational drift of the wild-type MCFD2^{wt} protein was largely a result of changes in the flexible loop (residues 102–113) rather than the unfolding of the α -helices.

In contrast, the secondary structure of the MCFD2^{D81H-V100D} mutant was progressively disrupted during the MD simulation. As shown in Fig. 3, the C α -RMSD values slowly increased as a function of time without achieving a plateau. The disruption started from the α -helix H4 region, with the helical secondary structure of the last residues disappearing after 1–2 ns, and spread into α -helix H3 (residues 114–128) and the EF-1-hand loop region. At the end of the MD simulation, part of α -helix H3 was destroyed (Fig. 4). The superimposition of the MCFD2 NMR structure with the averaged mutant structure obtained after the 50-ns MD simulations showed that the unfolding of the protein is started by the α -helix H4 (Fig. 2). The upper limit of the unfolding time would presumably increase further with longer simulations, since most of the changes in the properties after ~4 ns were gradual.

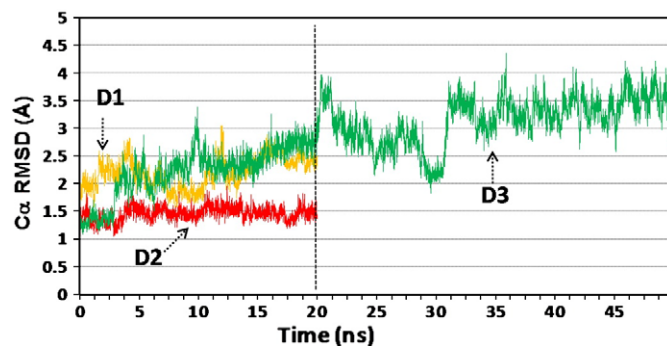


Fig. 3. MD-simulated C α -RMSD of the wild-type and mutated MCFD2 proteins. Trace D1 represents the C α -RMSD for the full-length MCFD2^{wt} protein. Trace D2 represents the C α -RMSD for the MCFD2^{wt} without the residues of the unstructured loop. Trace D3 represents the C α -RMSD for the MCFD2^{D81H-V100D} mutant without the residues of the unstructured loop.

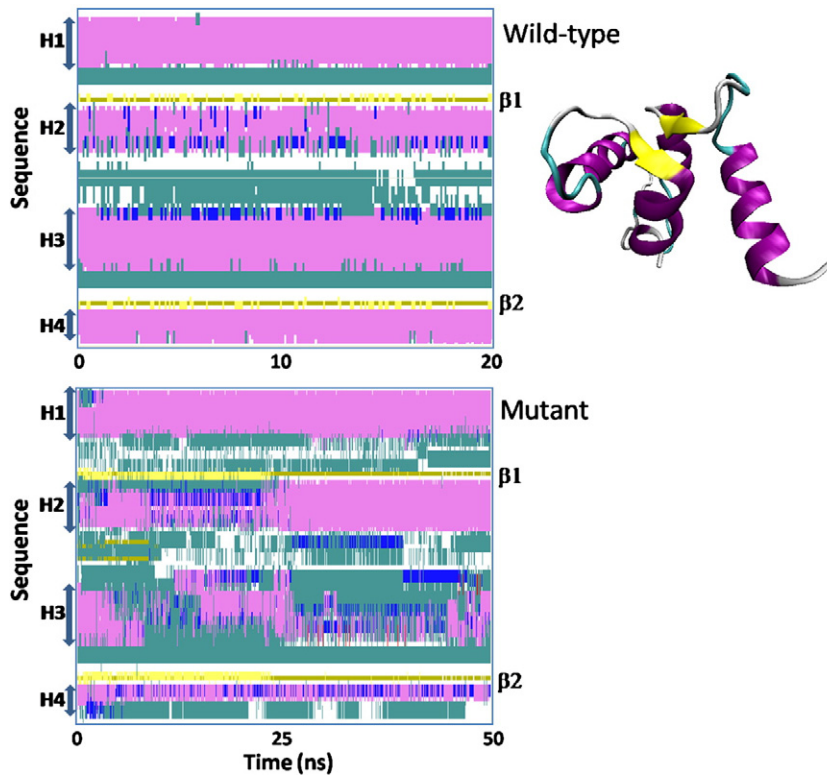


Fig. 4. Time evolution of the secondary structure of (Top) wild-type MCFD2 and (Bottom) mutant MCFD2^{D81H-V100D} proteins during the MD-simulated trajectory. The secondary structure colors are indicated on the 3D model (left).

The results from our large-scale simulations complement recent experimental results and clinical features and provide initial insight into the mechanism inducing the disruption of LMAN1/MCFD2

complex due to the MCFD2^{D81H-V100D} protein unfolding (Fig. 5). Taken together, the relatively large structural movement and the decrease stability of the α -helical and EF-1-hand domains of

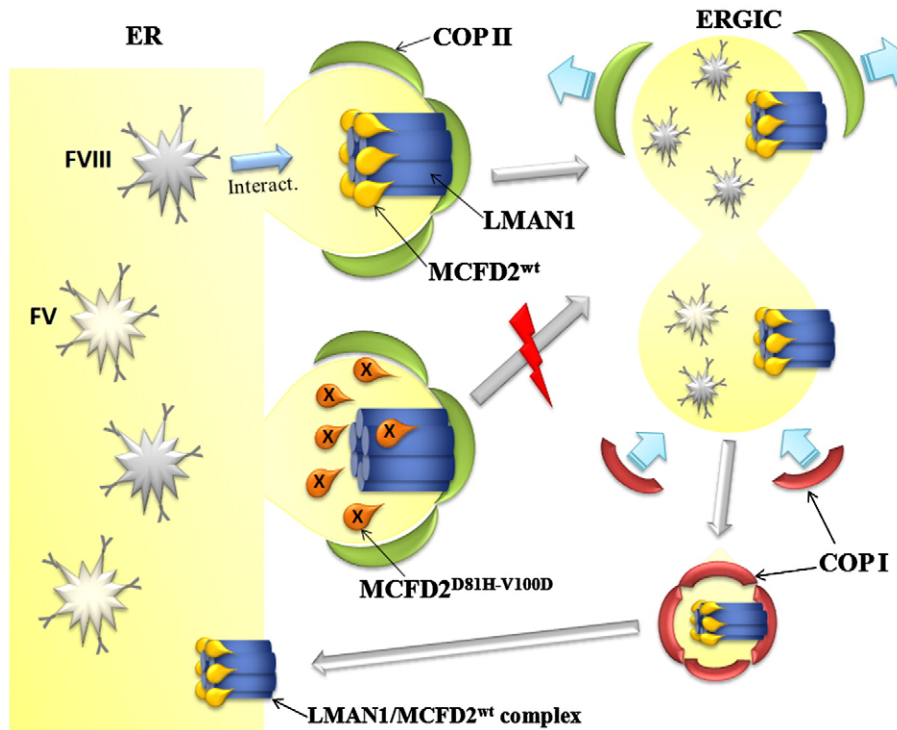


Fig. 5. The FV and FVIII cargo-protein transport pathways involving the LMAN1/MCFD2 complex. Cargo proteins (FV and FVIII) are packaged into COPII vesicles via interactions with LMAN1/MCFD2 complex. Vesicles fuse with each other to form the ERGIC, and cargo proteins are released. The LMAN1/MCFD2 complex is recycled back to ER from the ERGIC in COPI vesicles to participate in another round of cargo transport. Wild-type MCFD2^{wt} protein interact with LMAN1 (hexameric complex) in the ER lumen (1:1 stoichiometry). The unfolded state of MCFD2^{D81H-V100D} protein prevents the formation of LMAN1/MCFD2 complex and consequently the transport of FV or FVIII cargo proteins.

MCFD2^{D81H-V100D} protein may ultimately be expressed at the functional level as a form of F5F8D disease.

Acknowledgments

We wish to thank Drs. Mahrzia Ben Fadhel, Raja Marrakchi, Kaouther Zahra, Marta Spreafico, Chiraz Souissi Bouchlaka, Ines Khadimallah, Manel Kachoukh and Rayhana Zitoun for kindly helping us with this study.

References

- [1] J. Oeri, M. Matter, H. Isenschmid, et al., Congenital factor V deficiency (parahemophilia) with true hemophilia in two brothers, *Bibliotheca Paediatrica* 58 (1954) 575–588.
- [2] B. Zhang, M.A. Cunningham, W.C. Nichols, et al., Bleeding due to disruption of a cargo-specific ER-to-Golgi transport complex, *Nat. Genet.* 34 (2003) 220–225.
- [3] H.P. Hauri, F. Kappeler, H. Andersson, et al., ERGIC-53 and traffic in the secretory pathway, *J. Cell Sci.* 113 (2000) 587–596.
- [4] B. Zhang, M. Spreafico, C. Zheng, et al., Genotype-phenotype correlation in combined deficiency of factor V and factor VIII, *Blood* 111 (2008) 5592–5600.
- [5] E. Lindahl, B. Hess, D. van der Spoel GROMACS 3.0: a package for molecular simulation and trajectory analysis, *J. Mol. Model* 7 (2001) 306–317.
- [6] T. Zhang, A. Hamza, X.H. Cao, et al., A novel Hsp90 inhibitor to disrupt Hsp90/Cdc37 complex against pancreatic cancer cells, *Mol. Cancer Ther.* 7 (2008) 162–170.
- [7] J.E. Guy, E. Wigren, M. Svard, et al., New insights into multiple coagulation factor deficiency from the solution structure of human MCFD2, *J. Mol. Biol.* 381 (2008) 941–955.
- [8] J.J. Chou, S.P. Li, C.B. Klee, et al., Solution structure of Ca²⁺-calmodulin reveals flexible hand-like properties of its domains, *Nat. Struct., Biol.* 8 (2001) 990–997.

Hejer Elmahmoudi Abdallah
 Nejla Stambouli
 Mohamed Ben Amor
 Asma Jlizi
 Nejla Belhedi
 Rim Sassi
 Houssein Khodjetelkhal
 Adel Hamza*
 Amel Benammar Elgaaied*

*Laboratory of Genetics, Immunology and Human Pathology,
 Faculty of Sciences of Tunis, Tunis, Tunisia*

E-mail address: ahamz3@email.uky.edu (A. Hamza).

*Corresponding authors. Present address (A. Hamza):
 Department of Pharmaceutical Sciences, College of Pharmacy,
 University of Kentucky, Lexington, KY 40536, USA.

Emna Gouider
 Balkis Meddeb
 Raouf Hafsia
*Laboratory of Hematology, Aziza Othmana Hospital,
 Tunis, Tunisia*

10 November 2009

(Communicated by M. Lichtman, M.D.,
 16 November 2009)